P. G. Hodge, Jr.

Professor of Mechanics,
Department of Aerospace Engineering and Mechanics,
University of Minnesota,
Minneapolis, Minn. 55455
Hon. Mem. ASME

H. M. van Rij[2]

Engineer,
Netherlands Energy and Research Foundation,
Sichting Energieonderzoek Centrum,
Nederland, The Netherlands.

A Finite-Element Model for Plane-Strain Plasticity[1]

A finite-element model is proposed which allows for both straining within each element and slip between two elements. Basic equations are derived and are shown to almost completely uncouple into two constituent components: the conventional finite-element equations for continuous displacement fields and the "slip" equations which were recently derived for a model based on slipping of rigid triangles. The model is applied to the Prandtl punch problem and is shown to combine the best features of its two constituents.

1 Introduction

In an earlier paper [1] we pointed out that classical finite-element methods suffer from two potential drawbacks when applied to plane-strain problems of contained flow of an elastic/perfectly plastic material. On the one hand, plastic strain increments are incompressible, a condition which imposes severe constraints on the possible element configurations and may lead to very poor results [2]. Second, some continuum solutions of plasticity problems are known to exhibit discontinuities of tangential velocity across certain boundaries, and classical models cannot handle this feature.

In [1] we proposed a "slip model" which consisted of rigid triangular elements which were free to slide but not separate. Applied to a particular example, the slip model predicted good approximations to the yield-point load, collapse mechanism, and shape of the elastic displacement field. However, all results were obtained in terms of a fictitious elastic modulus which is essentially unknowable.

The present paper is concerned with a "combined model" which apparently has all of the advantages and none of the drawbacks of the classical and slip models taken separately. Further, the computations essentially reduce to a sequence of solutions for classical models and slip models so that the large body of knowledge available for the elastic/plastic classical model can be applied immediately, as can the experience gained in [1] with the slip model.

All three models are based on triangular elements. For simplicity of exposition and application we shall consider the regular array of right-isosceles triangular elements shown in Fig. 1. The kinematics of the classical model [3] are defined by the dimensionless nodal displacements (u_k, v_k). These displacements define a continuous, piecewise differentiable displacement field and a piecewise constant strain field over the entire domain. Fig. 2 shows the basic unit mechanisms u_k associated with a "small node" (Fig. 2(*a*)) and "large node" (Fig. 2(*b*)); the v_k mechanisms are similar.

As shown in [1], the kinematics of the slip model are defined by nodal rotations θ_k defined in Fig. 3. The resulting deformation field consists of infinitesimal rigid-body motions of the triangles accompanied by slip of one triangle relative to another.

The proposed combined model has three degrees of freedom at each interior node: a horizontal displacement u_k defined in Fig. 2, a similar

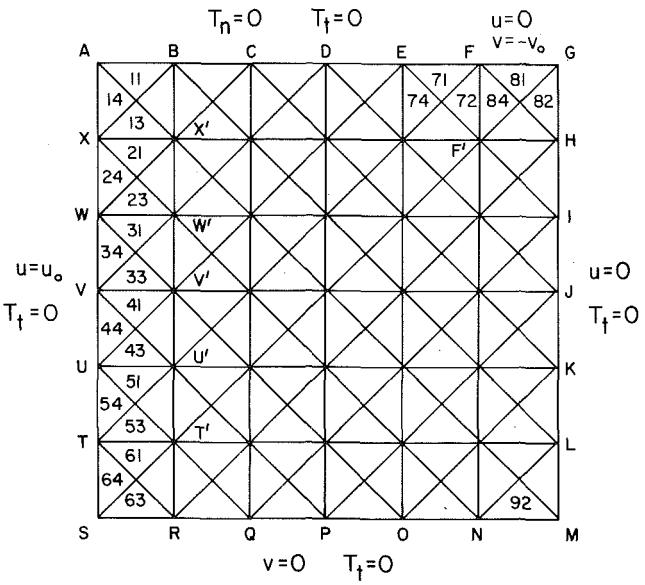

Fig. 1 Finite-element arrangement for Prandtl punch

---

[1] This research was sponsored by the Office of Naval Research and partially supported by the University of Minnesota Computer Center; the results are taken from a dissertation submitted to the University of Minnesota by one of the authors (H.V.R.) in partial fulfillment of the requirements for a Doctor of Philosophy degree.

[2] Formerly, Research Assistant, University of Minnesota, Minneapolis, Minn.

Contributed by the Applied Mechanics Division for presentation at the Winter Annual Meeting, New York, N.Y., December 2–7, 1979, of THE AMERICAN SOCIETY OF MECHANICAL ENGINEERS.

Discussion on this paper should be addressed to the Editorial Department, ASME, United Engineering Center, 345 East 47th Street, New York, N. Y. 10017, and will be accepted until December 1, 1979. Readers who need more time to prepare a Discussion should request an extension of the deadline from the Editorial Department. Manuscript received by ASME Applied Mechanics Division, June, 1978; final revision, February, 1979. Paper No. 79-WA/APM-19.

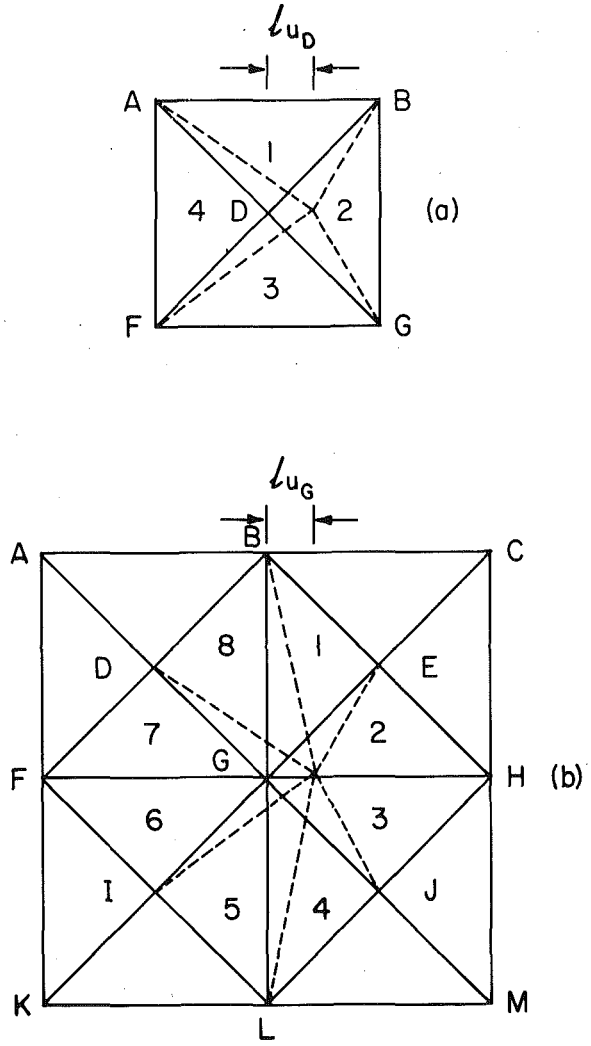

Fig. 2 Elementary horizontal mechanisms; (*a*) small node and (*b*) large node

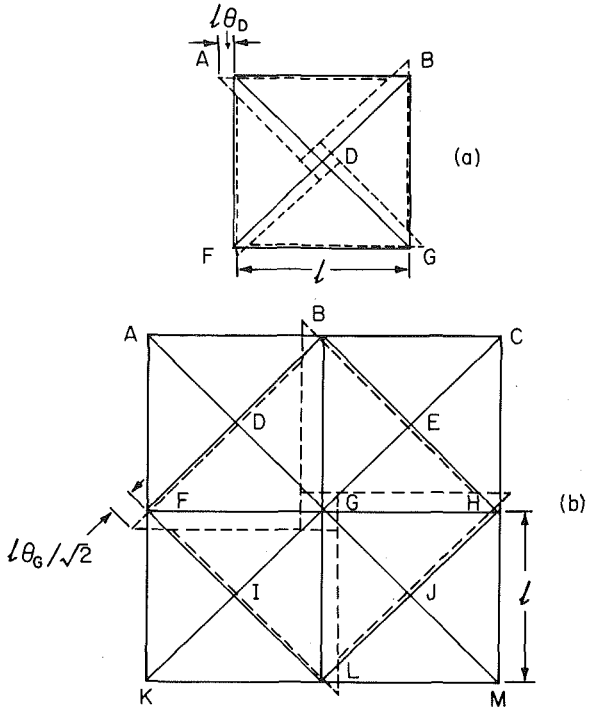

Fig. 3 Elementary slip mechanism; (*a*) small node and (*b*) large node

vertical displacement v_k, and a rotation θ_k defined in Fig. 3. We recall that in the classical model u_k and v_k can also be interpreted as the actual motion of node k. However, in the slip and combined models the rotation θ_k gives a different motion to each vertex at a node, so that the concept of "nodal displacement" has no direct physical significance.

The kinematics of the combined model are fully defined by Figs. 2 and 3; obviously they are the sum of the kinematics of the classical and slip models and there is no kinematic coupling of the two models.

The statics of each model can be obtained from Figs. 2 and 3 and the Principle of Virtual Work. If there are no body forces, then it is evident that the resulting static equations for each interior node will be homogeneous and linear, and that the combined model is simply the sum of the other two.

It remains then, to consider the constitutive equations and the boundary conditions, and we will do that in Sections 2 and 3, respectively. Section 2 will also list generic kinematic and static equations. Then in Section 4 we will examine in detail a specific boundary-value problem in order to clearly indicate the character of the proposed model, with particular reference to the close relation between it and the classical and slip models for the same problem. Section 5 will apply the model to an approximation to the Prandtl punch problem [5, 6]. The paper will conclude with a discussion of the merits of the model.

2 Basic Equations

We begin by reviewing the well-known equations for the classical model, follow with a summary of the slip-model equations from [1], and conclude by demonstrating that the slip-model constitutive equations are the only ones which must be modified before these equations can be applied to the combined model.

For the classical model the generalized displacements are the dimensionless nodal displacements

$$u_k = U_k/l \quad v_k = V_k/l \tag{1}$$

where l is the length of the triangle hypotenuse. These displacements determine a unique continuous piecewise-linear displacement field which leads to piecewise-constant strains. Taking these as generalized strains $\epsilon_x{}^\alpha$, $\epsilon_y{}^\alpha$, $\gamma_{xy}{}^\alpha$, we obtain for triangle ADB (triangle 1) in Fig. 2(*a*),

$$\epsilon_x{}^1 = u_B - u_A \qquad \epsilon_y{}^1 = v_A + v_B - 2v_D$$
$$\gamma_{xy}{}^1 = u_A + u_B - 2u_D + v_B - v_A \tag{2}$$

with similar expressions for the other elements.

Generalized stresses will be defined by

$$\sigma_x{}^\alpha = \frac{4}{l^2k}\int_{A^\alpha} \sigma_x(x, y)dA \tag{3}$$

etc., where k is the yield stress in shear. For any reasonable homogeneous material, constant strains will produce constant stresses so that (3) reduces to

$$(\sigma_x{}^\alpha, \sigma_y{}^\alpha, \tau_{xy}{}^\alpha) = (1/k)(\sigma_x, \sigma_y, \tau_{xy}) \tag{4}$$

If point D is the only node with a nonzero displacement in Fig. 2(*a*), then the internal work done in triangle ABD is

$$W_{\text{int}} = \int_{ABD} (\sigma_x\epsilon_x + \sigma_y\epsilon_y + \tau_{xy}\gamma_{xy})dA$$
$$= (kl^2/2)(-v_D\sigma_y{}^1 - u_D\tau_{xy}{}^1) \tag{5}$$

The total internal work done by a motion of point D is

$$W_{\text{int}} = (kl^2/2)[u_D(-\sigma_x{}^2 + \sigma_x{}^4 - \tau_{xy}{}^1 + \tau_{xy}{}^3) + v_D(-\sigma_y{}^1 + \sigma_y{}^3 - \tau_{xy}{}^2 + \tau_{xy}{}^4)] \quad (6)$$

If there is no force applied to node D, the internal work must vanish for all choices of u_D and v_D, hence we obtain the linear homogeneous static equations

$$(\sigma_x{}^2 - \sigma_x{}^4) + (\tau_{xy}{}^1 - \tau_{xy}{}^3) = 0 \quad (7a)$$

$$(\tau_{xy}{}^2 - \tau_{xy}{}^4) + (\sigma_y{}^1 - \sigma_y{}^3) = 0 \quad (7b)$$

associated with a generic small node. Similarly, at a large node, Fig. 2(*b*), we are led to

$$(\sigma_x{}^1 + \sigma_x{}^2 + \sigma_x{}^3 + \sigma_x{}^4) - (\sigma_x{}^5 + \sigma_x{}^6 + \sigma_x{}^7 + \sigma_x{}^8) + (\tau_{xy}{}^7 + \tau_{xy}{}^8 + \tau_{xy}{}^1 + \tau_{xy}{}^2) - (\tau_{xy}{}^3 + \tau_{xy}{}^4 + \tau_{xy}{}^5 + \tau_{xy}{}^6) = 0 \quad (7c)$$

$$(\tau_{xy}{}^1 + \tau_{xy}{}^2 + \tau_{xy}{}^3 + \tau_{xy}{}^4) - (\tau_{xy}{}^5 + \tau_{xy}{}^6 + \tau_{xy}{}^7 + \tau_{xy}{}^8) + (\sigma_y{}^7 + \sigma_y{}^8 + \sigma_y{}^1 + \sigma_y{}^2) - (\sigma_y{}^3 + \sigma_y{}^4 + \sigma_y{}^5 + \sigma_y{}^6) = 0 \quad (7d)$$

We consider an isotropic elastic/perfectly plastic material in plane strain. In each element the stresses and strains will be constant, so that the constitutive equations relating the generalized stresses and strains for element α are trivially derived from those for the continuum

$$f^\alpha = (\sigma_x{}^\alpha - \sigma_y{}^\alpha)^2/4 + (\tau_{xy}{}^\alpha)^2 \le 1 \quad \dot\lambda^\alpha \ge 0$$

$$\dot\sigma_x{}^\alpha = 2(G/k)[\dot\epsilon_x{}^\alpha + \nu(\dot\epsilon_x{}^\alpha + \dot\epsilon_y{}^\alpha)/(1-2\nu)] - \dot\lambda^\alpha(\sigma_x{}^\alpha - \sigma_y{}^\alpha)/2$$

$$\dot\sigma_y{}^\alpha = 2(G/k)[\dot\epsilon_y{}^\alpha + \nu(\dot\epsilon_x{}^\alpha + \dot\epsilon_y{}^\alpha)/(1-2\nu)] - \dot\lambda^\alpha(\sigma_y{}^\alpha - \sigma_x{}^\alpha)/2$$

$$\dot\tau_{xy}{}^\alpha = (G/k)\dot\gamma_{xy}{}^\alpha - 2\dot\lambda^\alpha\tau_{xy}{}^\alpha$$

$$\text{if} \quad f^\alpha < 1 \quad \text{or} \quad \dot f^\alpha < 0 \quad \text{then} \quad \dot\lambda^\alpha = 0$$

$$\text{else} \quad \dot\lambda^\alpha = (G/2k)[(\sigma_x{}^\alpha - \sigma_y{}^\alpha)(\dot\epsilon_x{}^\alpha - \dot\epsilon_y{}^\alpha) + \tau_{xy}{}^\alpha\dot\gamma_{xy}{}^\alpha] \quad (8)$$

For the slip model, the dimensionless generalized displacements are θ_D and θ_G defined in Figs. 3(*a*, *b*). A dimensionless generalized strain ω is defined for a generic edge PQ by

$$\omega_{PQ} = d_{PQ}l_{PQ}/l^2 \quad (9)$$

where d_{PQ} is the relative motion of the two triangles along PQ, defined as positive clockwise. As shown in [1], generalized strains are defined for each horizontal and vertical edge between nodes, but a single generalized strain is defined for each diagonal of a square. Thus the only nonzero strains associated with the elementary mechanisms in Figs. 3(*a*, *b*), respectively, are

$$\omega_{FG} = \omega_{GB} = \omega_{BA} = \omega_{AF} = \theta_D \quad \omega_{AG} = \omega_{BF} = -2\theta_D \quad (10a)$$

$$\omega_{FL} = \omega_{LH} = \omega_{HB} = \omega_{BF} = -\omega_{FG} = -\omega_{LG} = -\omega_{HG} = -\omega_{BG} = \theta_G \quad (10b)$$

Generalized strains may be related to continuum strains by regarding the edge as a rectangular domain of small thickness $l\delta$. In a general edge PQ the only nonzero strain is

$$\gamma = \omega_{PQ}l/(l_{PQ}\delta) \quad (11)$$

Since γ is constant, the only nonzero continuum stress is the constant τ and we define a generalized stress by

$$\tau_{PQ} = \lim_{\delta\to 0}\int_A \frac{\tau dA}{kll_{PQ}\delta} = \frac{\tau}{k} \quad (12)$$

Then the internal work done in edge PQ is

$$W_{\text{int}}{}^{PQ} = kl^2\tau_{PQ}\omega_{PQ} \quad (13)$$

Therefore, if no external work is done in the mechanism motions in Fig. 3, the linear homogeneous static equations are easily obtained

$$\tau_{FG} + \tau_{GB} + \tau_{BA} + \tau_{AF} - 2\tau_{AG} - 2\tau_{BF} = 0 \quad (14a)$$

$$\tau_{FL} + \tau_{LH} + \tau_{HB} + \tau_{BF} - \tau_{FG} - \tau_{LG} - \tau_{HG} - \tau_{BG} = 0 \quad (14b)$$

Formal combination of the Prandtl-Reuss flow law for pure shear with equations (11) and (12) leads to the constitutive equation for edge PQ

$$\tau_{PQ}{}^2 \le 1 \quad (15a)$$

$$\text{if} \quad \tau_{PQ}{}^2 < 1 \quad \text{or} \quad \tau_{PQ}\dot\tau_{PQ} < 0 \quad (15b)$$

$$\text{then} \quad \dot\tau_{PQ} = (Gl/kl_{PQ}\delta)\dot\omega_{PQ} \quad (15c)$$

$$\text{else} \quad \dot\tau_{PQ} = 0 \quad (15d)$$

Now, equation (15*c*) is not usable as written, since it contains the "thickness" δ of the edge—which must tend to zero. For the slip model this dilemma is resolved by defining a "slip modulus."

$$G' = G/\delta \quad (16)$$

As shown in [1], this procedure enables us to obtain complete elastic/plastic stress distributions and to obtain displacement fields in terms of the unknown (and unknowable) constant G'.

However, for the combined model considered here, the shear modulus G is necessary for equations (8) to have meaning, and hence it cannot be allowed to tend to zero as is implied by equation (16). Therefore, we must resolve our dilemma in a different way by defining new alternative kinematic variables $\bar\theta_P$, etc., by

$$d_{PQ} = \bar d_{PQ}\delta \quad \omega_{PQ} = \bar\omega_{PQ}\delta \quad \theta_P = \bar\theta_P\delta \quad (17)$$

Equations (15) then become

$$\tau_{PQ}{}^2 \le 1 \quad (18a)$$

$$\text{if} \quad \tau_{PQ}{}^2 < 1 \quad \text{or} \quad \tau_{PQ}\dot\tau_{PQ} < 0 \quad (18b)$$

$$\text{then} \quad \dot\omega_{PQ} = 0 \quad \text{and} \quad \dot\tau_{PQ} = (Gl/kl_{PQ})\dot{\bar\omega}_{PQ} \quad (18c)$$

$$\text{else} \quad \dot\tau_{PQ} = 0 \quad (18d)$$

If (18*b*) is satisfied, there will be no slip. However, in view of equation (17), zero strain is compatible with nonzero alternative variables $\bar\omega_{PQ}$ so that we still have a nontrivial set of slip equations. In particular, $\dot\tau_{PQ}$ and hence τ_{PQ} can be determined so that the continued validity of (18*b*) can be tested. On the other hand, if (18*b*) is violated, we bypass (18*c*) to obtain directly the simple (18*d*). Since this equation gives no kinematic information it is compatible with either zero ω_{PQ} and nontrivial $\bar\omega_{PQ}$, or with nonzero ω_{PQ} in which case the alternative kinematic variables are discarded. The choice between these two alternatives will depend upon the problem as a whole, and will be discussed in later sections.

With the exception of the foregoing discussion of the constitutive equations, it is clear that the defining equations for the classical and slip parts are independent and hence may be added to obtain the combined model. Therefore, for the combined model the kinematics are governed by equations (2), (10) and (17), the statics by (7) and (14), and the constitutive behavior by (8) and (18).

3 Boundary-Value Problem

Boundary conditions are most easily discussed in terms of a specific example. To this end we consider the problem shown in Fig. 1. For any of the three models local constitutive equations and strain-displacement equations will exactly match the unknown generalized strains and stresses. Therefore, in order to balance the total system of equations and unknowns, there must be one equilibrium equation for each generalized displacement.

For the classical model, each of the interior nodes has two displacement unknowns u_i and v_i, and the same number of equations, equations (7). On the boundary, $u = 0$ for nodes G through M, $v = 0$ for nodes M through S, and

$$u_S = u_T = u_U = u_V = u_W = u_X = u_A = u_0 \quad v_F = v_G = -v_0 \quad (19)$$

For the remaining 10 unknown u's and 15 unknown v's we can use equations (7c) and (7d), respectively, keeping only those stress terms which correspond to triangles in the domain.

Applying the principle of virtual work to motions defined by u_0 and v_0, respectively, we obtain

$$T_2 = (1/24)\sum_{1}^{6}[-(\sigma_x{}^{i1} + \sigma_x{}^{i3} + 2\sigma_x{}^{i4}) + (\tau_{xy}{}^{i1} - \tau_{xy}{}^{i3})] \quad (20a)$$

$$T_1 = (1/4)[-(\tau_{xy}{}^{71} + \tau_{xy}{}^{72} + \tau_{xy}{}^{82} - \tau_{xy}{}^{84}) - (\sigma_y{}^{71} + \sigma_y{}^{72} + 2\sigma_y{}^{81} + \sigma_y{}^{82} + \sigma_y{}^{84})] \quad (20b)$$

where kT_2 and kT_1 are, respectively, the forces per unit length pushing SA to the right and FG down. If T_2 is given, (20a) is the necessary equation for the additional unknown u_0; if u_0 is given, (20a) defines the necessary force T_2. Similar interpretations apply to T_1 and equation (20b).

For the slip model, we first note that if all θ_i were equal, the entire domain would remain unchanged, so that we may arbitrarily set $\theta_M = 0$. It then follows from Fig. 1 (see [1] for details) that all of θ_G through θ_S vanish,

$$\theta_T = \theta_U/2 = \theta_V/3 = \theta_W/4 = \theta_X/5 = \theta_A/6 = 2u_0 \quad \theta_F = -2v_0 \quad (21)$$

and θ_B, θ_C, θ_D, and θ_E are four new variables.

As shown in [1] boundary mechanisms are somewhat simpler than interior ones, so that the equilibrium equation for node B is

$$\tau_{AX'} + \tau_{CX'} - \tau_{BX'} = 0$$

with similar expressions for nodes C, D, and E. The mechanism motion for v_0 involves only node F and leads to

$$2T_1 = -\tau_{EF'} - \tau_{GF'} + \tau_{FF'} + \tau_{FG}/2 \quad (22a)$$

whereas the mechanism motion for u_0 involves all of the nodes on the left and leads to

$$3T_2 = (\tau_{ST'} + \tau_{UT'} - \tau_{TT'}) + 2(\tau_{TU'} + \tau_{VU'} - \tau_{UU'}) + 3(\tau_{UV'} + \tau_{WV'} - \tau_{VV'}) + 4(\tau_{VW'} + \tau_{XW'} - \tau_{WW'}) + 5(\tau_{WX'} + \tau_{AX'} - \tau_{XX'}) + 6\tau_{XB} \quad (22b)$$

As with the classical model, equations (22) may be used to find displacements if forces are given or to define forces for given u_0 and/or v_0.

For the combined model, we must interpret the prescribed boundary motions in terms of permissible mechanism motions. However, before doing this, we observe that not all of the generalized displacements in the total domain are independent. As with the slip model, we may arbitrarily set $\theta_M = 0$. Further, we observe from Fig. 3 that the combination of motions $\theta_A = \theta_B = 2\lambda$, $\theta_D = \lambda$, $u_D = -\lambda$ results in zero motion for any λ, so that one of the variables is not independent. A similar argument can be applied to any rectangular domain in both the horizontal and vertical direction. Therefore in Fig. 1 we arbitrarily set $\theta_L = \theta_N = 0$. We note that these three arbitrary conditions are inherent in our choice of kinematic variables and are not related to a rigid-body motion of the entire domain.

For the problem in Fig. 1 it is not difficult to show [4] that if we replace u_0 and v_0 by u_{0c} and v_{0c} in equations (19) and by u_{0s} and v_{0s} in (21), then these four new variables are related by

$$u_{0c} + u_{0s} = u_0 \quad v_{0c} + v_{0s} = v_0 \quad (23)$$

The total system of equations is still balanced since we can use all four of equations (20) and (22) for the two additional variables T_1 and T_2.

Examining the boundary-value problems for the three models, we see that the combined model equations are the totality of those for the other two models except for the equations based on motions u_0 and v_0. Thus a combined model problem can be almost completely uncoupled into separate classical and slip model problems. We shall discuss the details of this phenomenon in the next section.

4 Solution

We consider a specific case of the boundary-value problem defined in Fig. 1 where $u_0 = 0$ and v_0 is slowly increased from zero.

For v_0 sufficiently small, all elements will be elastic. Therefore all classical elements will follow the first branch in equations (8) and all slip elements will follow the first in equations (18). Thus equation (18c) will lead to the vanishing of *all* real slip displacements, specifically including u_{0s} and v_{0s}. Thus $u_{0c} = 0$ and $v_{0c} = v_0$, and the combined problem is identical to the classical one with prescribed displacement conditions. Therefore, it can be solved without reference to equations (20) which are then available to determine T_1 and T_2. But with T_1 and T_2 known, the remaining combined model equations are identical to those of the slip model with alternative kinematic variables and prescribed loads. Therefore, in the *elastic range* we can solve the combined model by solving the classical and slip models in order.

Now for some critical value of v_0, some element must reach yield and from here on all equations must be written in rate form. If a triangle yields we must take the second branch in (8), but the method of analysis remains unchanged. When the first slip element yields, either before or after yielding of any triangle elements, the second branch of equations (18) must be used for that element. However, it is not possible for any one $\dot{\omega}_{PQ}$ to be nonzero, so that we must continue to use the alternative kinematic slip variables. Thus, at this stage, we are in the *uncoupled plastic range* where the combined model is solved by sequential solution of the classical and slip models.

As v_0 is still further increased, more and more elements will reach yield and require the second branch in equations (8) or (18). Eventually, sufficient slip elements will reach yield so that, if u_{0s} and v_{0s} are both regarded as free variables, a combined mechanism motion of the slip model would be possible. Since all rotation displacements in this motion can be expressed in terms of u_{0s} and v_{0s}, the mechanism will be defined by some relation

$$\alpha\dot{u}_{0s} + \beta\dot{v}_{0s} = 0 \quad (24)$$

where α and β are not both zero. It turns out that no external work is associated with this mechanism, so that

$$6\dot{T}_2\dot{u}_{0s} + \dot{T}_1\dot{v}_{0s} = 0 \quad (25)$$

hence

$$\alpha\dot{T}_1 - 6\beta\dot{T}_2 = 0 \quad (26)$$

For further increase in v_0, the boundary displacements for the classical problem are now defined by

$$\dot{u}_{0c} = -\dot{u}_{0s} \quad \dot{v}_{0c} = \dot{v}_0 - \dot{v}_{0s} \quad (27)$$

Additional equations for the two new unknowns $\dot{u}_{0s}$ and $\dot{v}_{0s}$ are provided by (24) and by the substitution of (20) in (26).

Once the classical problem is solved, $\dot{u}_{0s}$ and $\dot{v}_{0s}$ will be known, hence so will those $\dot{\theta}_i$ which are involved in the mechanism. The remainder of the slip model can still be solved in terms of the alternative kinematic variables. In obtaining this solution we can arbitrarily set one of the external alternative kinematic variables equal to zero, say $\dot{\bar{u}}_{0s}$, since the forces will automatically satisfy (26).

Further increase of v_0 will lead to more elements becoming plastic. However, until a second mechanism forms we remain in the *partly coupled plastic range* where the two parts are coupled only by equations (24) and (26) and hence may still be solved sequentially.

The next critical value of v_0 occurs when an independent second slip mechanism forms. Now $\dot{u}_{0s}$ and $\dot{v}_{0s}$ are independent variables not subject to (24). Since neither of these independent mechanisms will do net work,

$$\dot{T}_1 = \dot{T}_2 = 0 \quad (28)$$

and we have reached the *yield-point load*. Further increase in load is impossible for a perfectly plastic material in equilibrium.

Conceivably, the classical model alone could activate a yield-point mechanism while in the uncoupled range, or a mechanism could be

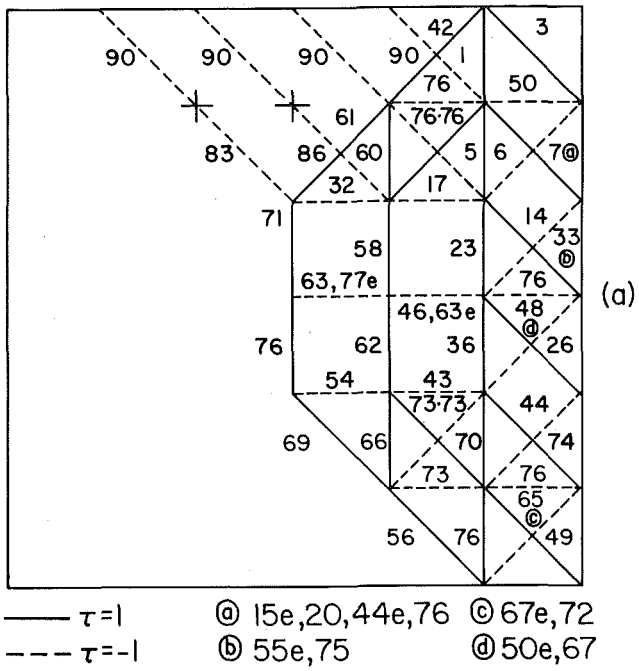

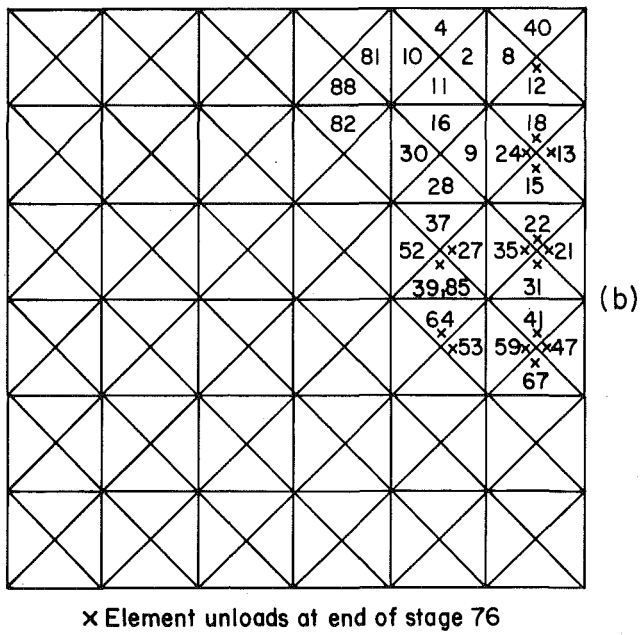

Fig. 4 Yielding sequence for Prandtl punch; (*a*) edges and (*b*) triangles

formed in the partly coupled range; in the examples considered, however, this was never the case.

Three complications to the qualitative description just given may occur. In the first place, even though v_0 increases monotonically, some elements may unload. Thus, after using the second branch in equations (8), a check must be made that $\dot{\lambda}^\alpha$ is non-negative. Similarly, if (18*d*) is used, $\dot{\omega}_{PQ}$ or $\dot{\varpi}_{PQ}$ must have the same sign as τ_{PQ}. Any element or elements where these requirements are not met must be switched to the other branch.

Second, the plastic solution to (8) for a triangle should satisfy the nonlinear equation $\dot{f} = 0$. Instead, it satisfies a linear condition equivalent to moving along a tangent to the surface $f = 1$, thus resulting in $\dot{f} > 0$. In order to keep the resulting error from growing too large, it is desirable to stop a stage whenever the change in f exceeds, say, 0.001, and to recompute the stress terms that appear in equations (8).

Finally, in some stages a lack of uniqueness occurs for the kinematical slip variables. This phenomenon was found in [1] for the slip model. At least in the uncoupled range, it is less disturbing here than in [1], since it involves only the alternative kinematic slip variables and the true slip remains uniquely zero.

We shall comment on all three of these complications more fully in relation to the example in the next section.

5 Example

A computer program was written to implement the three models and was used to solve the problem illustrated in Fig. 1 with $u_0 = 0$. An elastic/perfectly plastic material is placed in a perfectly lubricated box and indented with a rigid punch. This problem, which was considered in Section 4, is a finite domain approximation to the Prandtl problem [5, 6] of a rigid rough punch indenting a semi-infinite perfectly plastic material under conditions of plane strain. Details of the solution and a discussion of the computer program may be found in [4].

The slip model solution [1] is independent of Poisson's ratio; for the classical and combined model we took $\nu = 0.3$.

The yielding sequence of the edges and the triangles is shown in Fig. 4. In the uncoupled range the classical part of the solution is exactly the same for the classical and combined models. However, the slip part of the solution with the combined model is not identical with that of the slip model [1], since the stress solution interacts with the reaction forces of the classical part, even in the absence of slip. As might be expected, these differences grow as the load increases. A comparison of Fig. 4(*a*) and results from [1] shows that the first four edges to yield in the slip model are the first four to yield in the same order in the slip part of the combined model. The first eight edges to yield in the slip model are among the first nine, but in different order, to reach the yield stress in the slip part of the combined model. However, the ninth edge to yield in the slip model is only the 14th to reach yield in the slip part of the combined model, and the tenth yielding edge in the slip model is the 23rd in the slip part of the combined model.

As in the slip model solution, more than one edge may reach yield at the same time, as in stages 73, 76, and 90. In this example we never find two triangles reaching yield at the same time, although the phenomenon could certainly occur. However, at the end of stage 67 we find both one triangle and one edge reaching yield. None of the aforementioned coincidences cause any computational difficulty.

We also find that several stages are ended by an increase in f of 0.001. Specifically, this happens to end stages 45, 51, and 68 in the uncoupled range.

Load deflection curves for the three models are shown in Fig. 5. It is interesting to note than even though edge yielding in the uncoupled range does not influence the load deflection curve, the elastic limit of the combined model occurs at $T_1 = 2.52$, $v_0 = 1.92\ G/k$ when edge FF' reaches yield, whereas the fully elastic range in the classical model is terminated when triangle 72 yields at $T_1 = 2.76$ and $v_0 = 2.10\ G/k$.

At the end of stage 73 we find two undetermined rotation variables in the lower right corner. Although this nonuniqueness of alternative kinematic variables is a computational nuisance, it does not affect any of the stress variables or real kinematic variables, and does not lead to coupling between the classical and slip parts.

At the end of the stage 76, eight edges yield and produce several independent slip mechanisms of the true kinematic slip variables. However, all mechanisms involve the same motion at the boundaries, and equations (24) and (26) become, respectively,

$$\dot{v}_{0s} = 6\dot{u}_{0s} \quad \dot{T}_1 + \dot{T}_2 = 0 \tag{29}$$

As described in Section 4, we enter a new phase of the solution, where we have one interacting force between the classical part and the slip part. As a consequence the loading conditions of the classical part change. This change has a dramatic effect on the behavior of the triangular elements in that more than half of the elements which were

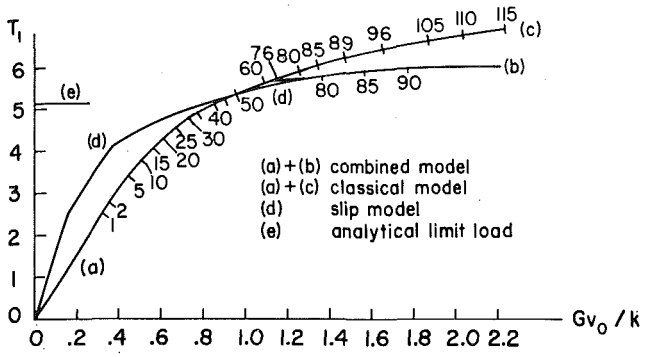

Fig. 5 Load-displacement curve for Prandtl punch

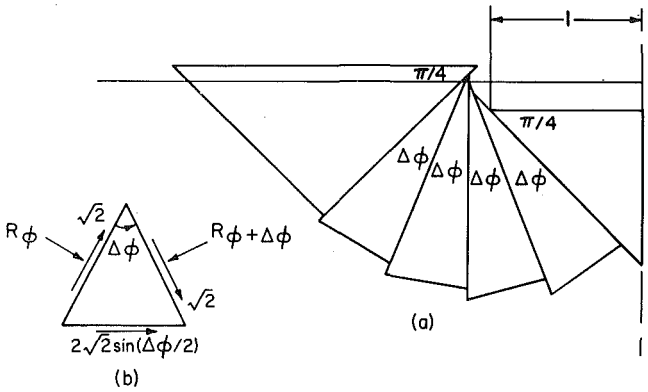

Fig. 6 Alternative element arrangement

yielding at the end of stage 76 (17 out of 29), now start to unload. These elements are indicated by asterisks in Fig. 4(*b*).

Fig. 5 shows that in this phase the load-deflection curve is no longer the same as the classical model due to the slip in the domain. Computation in this phase continues until the end of stage 90 when four simultaneously yielding edges cause limit load conditions. The limit load and the collapse mechanisms are the same as we found in [1] for the Prandtl rough punch with the slip model.

Also shown in Fig. 5 is the continuation of the load deflection curve for the classical model up to stage 115 when the load was about 14 percent above the yield-point load for the combined model. Further computation up to stage 153 increased the load to about 30 percent above the combined yield-point load and caused plastic flow in more than half the triangles, but still did not produce a yield-point mechanism. This phenomenon will be commented on in the final section.

6 Conclusions

We begin this section by summarizing some of the results for the three different models as applied to the Prandtl punch problem considered in Section 5. The classical model provides a well-defined elastic solution which agrees well with an analytical solution for a semi-infinite domain obtained by Green and Zerna [7]. Plastic regions develop in what appears to be a reasonable sequence with no unloading up to a load of about 7.25. As shown in [4], the computer program appears to become unstable above this point, and it does not predict a limit load. However, the theorems of limit analysis may be applied directly to this model [4, Appendix C] and they show that $T_1 = 7.23$ is the true limit load for the model.

The slip model gives only relative displacements, but these agree well with the analytical solution [7]. It predicts a limit load of 6.00, which is a reasonable upper bound on the true value of 5.14 [5, 6]. It provides many possible collapse mechanisms, one of which agrees well with the analytical one [1].

The combined model agrees exactly with the classical one up to $T_1 = 5.7$, gives exactly the same collapse load $T_1 = 6.00$ and mechanisms as the slip one, and provides a transition solution between these two which appears reasonable.

We note that all three models give limit loads above the true value. This is to be expected since each model is based on a kinematically admissible field for the continuum. An earlier slip model proposed by Frémond and Salençon [8] is only admissible in an "average" sense and hence does not provide true bounds.

Bars with notches in one or both sides and the Prandtl problem with a smooth punch were also considered in [4], with similar results. Based on this limited experience it appears that the combined model gives results which combine the best features of the other two.

The computations were carried out on a CDC Cyber 74. The total CPU times were approximately 30, 80, and 130 sec for the slip, classical, and combined models, respectively. A more meaningful comparison is the time per degree of freedom which was, respectively, 0.44, 0.55, and 0.62 sec for the three models. Unquestionably, more efficient programmers could reduce these times substantially, but their relative magnitudes are probably meaningful. Thus, on either a total or degree-of-freedom basis, the combined model is the most time-consuming. However, in view of the fact that neither the classical nor slip models provide an adequate complete elastic-plastic history, it is important to note that the combined-model time is only slightly more than the sum of the other two.

Some interesting questions remain to be answered. Two of the most important ones concern convergence to the true solution, and the partial lack of uniqueness mentioned earlier.

Since convergence of the classical model has been well studied, we restrict our remarks to the slip model. It would be desirable to examine the solution as the number of elements is increased and to compare the sequence so obtained with the continuum solution. This topic is one of continuing investigation and no specific results are available yet. However, with a different arrangement of triangles specifically chosen for the example in Section 5, convergence to the limit load can be explicitly demonstrated. To this end we consider the triangle arrangement in Fig. 6.

The limit load for any finite number n of wedge-triangles can be explicitly calculated [4, Chapter 3]

$$-T_1 = 2 + 4n\tan\frac{\pi}{4n} \tag{30}$$

which converges to the continuum limit load of $2 + \pi$ as n tends to infinity.

For a perfectly plastic structure at yield point it is well known that the magnitude of deformation must be nonunique and there are many examples of structures whose yield-point mechanisms have many independent degrees of freedom. However, although the present model is the first known example which exhibits more than one degree of freedom below the yield-point load, an investigation currently in progress [9] indicates that the phenomenon may also occur in simple truss and frame problems. Meanwhile, several facts concerning this situation are worth mentioning

1 The stresses and stress rates are all unique.

2 All velocities associated with external work are unique.

3 Explicit finite bounds are available on all nonunique kinematic variables.

4 Nonunique strain rates are associated only with plastic stresses.

5 There are no major computational difficulties in obtaining values for all unique quantities and bounds for all nonunique ones.

References

1 van Rij, H., and Hodge, P. G., Jr., "A Slip Model for Finite-Element Plasticity," ASME JOURNAL OF APPLIED MECHANICS, Vol. 45, 1978, pp. 527–532.

2 Nagtegaal, J. C., Parks, D. M., and Rice, J. R., "On Numerically Accurate Finite-Element Solutions in the Fully Plastic Range," *Comp. Meth. Applied Science and Engineering*, Vol. 4, 1974, pp. 153–177.

3 Turner, M. J., et al., "Stiffness and Deflection Analysis of Complex Structures," *Journal of the Aerospace Sciences*, Vol. 23, 1956, pp. 805–823.

4 van Rij, H., and Hodge, P. G., Jr., "Finite-Element Models With Velocity Discontinuities," AEM Report H1-21, University of Minnesota, June 1978.

5 Prandtl, L., "Ueber die Herte plastischer Koerper," *Goettinger Nachr, Math-Phys,* K1 1920, 1920, pp. 74–85.

6 Prager, W., and Hodge, P. G., Jr., *Theory of Perfectly Plastic Solids,* Wiley, New York, 1951 (Xerox University Microfilms, OP69234).

7 Green, A. E., and Zerna, W., *Theoretical Elasticity,* Clarendon, Oxford, 1954.

8 Frémond, M., and Salençon, J., "Limit Analysis by Finite-Element Methods," *Proceedings, Symposium on Plasticity and Soil Mechanics,* Cambridge, England, September 13–15, 1973, pp. 297–309.

9 White, D. L., and Hodge, P. G., Jr., "Examples of Nonuniqueness in Contained Plastic Deformation," AEM Report H1-24, University of Minnesota, July 1979.